

Coherent Population Trapping Combined with Cycling Transitions for Quantum Dot Hole Spins Using Triplet Trion States

Samuel G. Carter^{1,*}, Stefan C. Badescu², Allan S. Bracker¹, Michael K. Yakes^{1,†}, Kha X. Tran,³
 Joel Q. Grim¹ and Daniel Gammon¹

¹Naval Research Laboratory, 4555 Overlook Avenue SW, Washington, D.C. 20375, USA

²Air Force Research Laboratory, Sensors Directorate, Wright Patterson Air Force Base, Ohio 45433, USA

³NRC Research Associate at the Naval Research Laboratory, 4555 Overlook Avenue SW, Washington, D.C. 20375, USA



(Received 8 September 2020; revised 7 December 2020; accepted 9 February 2021; published 8 March 2021)

Optical spin rotations and cycling transitions for measurement are normally incompatible in quantum dots, presenting a fundamental problem for quantum information applications. Here we show that for a hole spin this problem can be addressed using a trion with one hole in an excited orbital, where strong spin-orbit interaction tilts the spin. Then, a particular trion triplet forms a double Λ system, even in a Faraday magnetic field, which we use to demonstrate fast hole spin initialization and coherent population trapping. The lowest trion transitions still strongly preserve spin, thus combining fast optical spin control with cycling transitions for spin readout.

DOI: 10.1103/PhysRevLett.126.107401

One of the most attractive features of self-assembled quantum dots (QDs) is their strong coupling to light, which makes them excellent photon emitters and also allows for fast optical manipulation of spin states. The ideal energy level system for optical control of the ground state spin is a Λ system in which both spin states couple to one excited state. The double Λ system shown in Fig. 1(b) is commonly achieved for singly charged QDs by applying a magnetic field perpendicular to the optical axis (Voigt geometry). This charged exciton (trion) system has been used to demonstrate optical spin initialization [1], ultrafast spin rotations [2,3], and coherent population trapping (CPT) [4–7]. For spin readout, however, a cycling transition is desired that results in the emission of many photons without changing the spin state. This has been accomplished for singly charged QDs by applying a magnetic field parallel to the optical axis (Faraday geometry), giving a double two-level system shown in Fig. 1(a), with a demonstration of single-shot spin readout [8].

Achieving both types of energy level systems for QDs in one geometry has been quite challenging, as the requirements for spin control and readout are conflicting. Some progress has been made with QDs in photonic crystal cavities and waveguides that enhance one set of transitions polarized with the cavity and inhibit the other set, making one set useful for initialization and the other for readout [9–12]. This technique requires a strong Purcell effect and alignment of the transition polarization with the cavity. Other approaches have been to use a spin selective ac Stark shift to optically change the energy level structure [13] or to make use of light-hole excitons [14–16]. There have also been efforts with pairs of coupled QDs, which have additional degrees of freedom that allow both Λ systems

for control and cycling transitions for readout [17,18]. This system, however, is more difficult to produce.

In this Letter, we report a new, simple approach to this challenge for a hole spin in a single QD using trion states in which one hole is in an excited orbital (often called “hot” trions). In a Faraday magnetic field, the lowest trion states form the well-known double two-level system in Fig. 1(a) with two cycling transitions [8,19]. The next optical transitions involve exciting an electron in the lowest orbital (e_0) and a hole in the first excited orbital (h_1). Using photoluminescence excitation (PLE) spectroscopy, we find that these triplet transitions can be very sharp ($\sim 8\text{--}10\ \mu\text{eV}$), and one particular triplet forms a double Λ system in a Faraday magnetic field [see Fig. 1(b)]. This happens because transitions that normally would be forbidden by spin selection rules become allowed due to spin-orbit

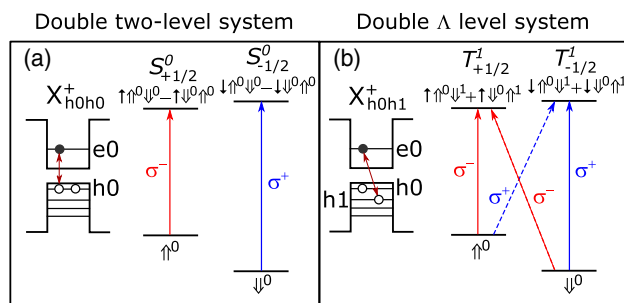


FIG. 1. (a) Double two-level system for the s -shell charged exciton in a Faraday magnetic field. (b) Double Λ system for a hot trion with one hole in an excited orbital in a Faraday magnetic field. Electron (hole) spins in e_0 (h_0) are represented by \uparrow (\uparrow^0), and a hole spin in h_1 is represented by \uparrow^1 .

coupling for a hole in higher orbitals. We use this Λ system to demonstrate fast hole spin initialization as well as CPT. This system provides for both efficient readout and fast optical control and also has the advantage of improved coherence of the hole spin over an electron spin, due to a weaker hyperfine interaction [5,20–24].

The InGaAs QDs are grown by molecular beam epitaxy on an n -doped GaAs substrate within a distributed Bragg reflector planar cavity (see Supplemental Material [25]). A vertical n - i - p - i - p diode within the cavity is used to charge the QD with a single hole. Experiments are performed between 2.8 and 5 K, at biases near the transition from one hole to two holes in order to vary the spin relaxation rate [30], either preventing or allowing optical pumping of the hole spin.

The states considered here and their fine structure are shown in Fig. 2(a). The ground state has one hole in the lowest orbital (h_0). The lowest trion state ($X_{h_0h_0}^+$) has two holes in h_0 and an electron in e_0 . The hot trion state ($X_{h_0h_1}^+$) has one hole in h_1 , another hole in h_0 , and the electron in e_0 . The e_0 , h_0 , and h_1 spins are represented by \uparrow , \uparrow^0 , and \uparrow^1 , respectively. The holes should be primarily heavy holes with $m_j = \pm 3/2$. For $X_{h_0h_0}^+$ the holes must form a spin singlet, giving two states $S_{\pm 1/2}^0$ with different electron spin projections. The fine structure of hot trion states has been explained in previous studies [31–37]. For $X_{h_0h_1}^+$ the holes can be in a singlet state or triplet states split by the isotropic hole-hole exchange energy Δ_{hh} . These trion states are labeled by $S_{m_f}^1$ and $T_{m_f}^1$, where $m_f = m_s + m_j$ is the total spin projection for the electron (m_s) and two holes (m_j). As has been reported previously, anisotropy in the hole-hole exchange interaction results in a shift δ_{hh} of the $m_j = 0$ triplet $T_{\pm 1/2}^1$ relative to $m_j = \pm 3$ triplets ($T_{\pm 5/2}^1$ and $T_{\pm 7/2}^1$), as well as shifts of the singlet $S_{\pm 1/2}^1$ [33]. The electron-hole exchange interaction further splits $T_{\pm 5/2}^1$ and $T_{\pm 7/2}^1$ by $2\Delta_{eh}$, which is much weaker than Δ_{hh} . Asymmetric electron-hole exchange is neglected. Each state is doubly degenerate at zero magnetic field.

PLE spectroscopy is performed by tuning the laser through the $X_{h_0h_1}^+$ transitions and measuring emission from $X_{h_0h_0}^+$ with a CCD spectrometer. In Fig. 2(b), the emission spectrum of $X_{h_0h_0}^+$ at $B = 0$ T shows a single main line. The weak, lower energy line comes from X^{2+} . Figure 2(c) plots the PLE spectrum of the next transitions of the QD, integrating emission from $S_{\pm 1/2}^0$, showing three sharp triplet lines ~ 3 meV below a broader singlet line. From the transition energies, we obtain $\Delta_{hh} \sim 3$, $\delta_{hh} = 0.605$, and $\Delta_{eh} = 0.234$ meV. From the singlet-triplet structure, we infer that the two holes must be in different orbitals, and the small energy separation from $X_{h_0h_0}^+$ indicates that the electron must be in e_0 . The triplet transition linewidths are 8–10 μ eV, and the singlet transition linewidth is 52 μ eV. Higher energy PLE lines are also observed for this QD (not shown) that have similar singlet-triplet patterns but broader linewidths. These lines are assigned

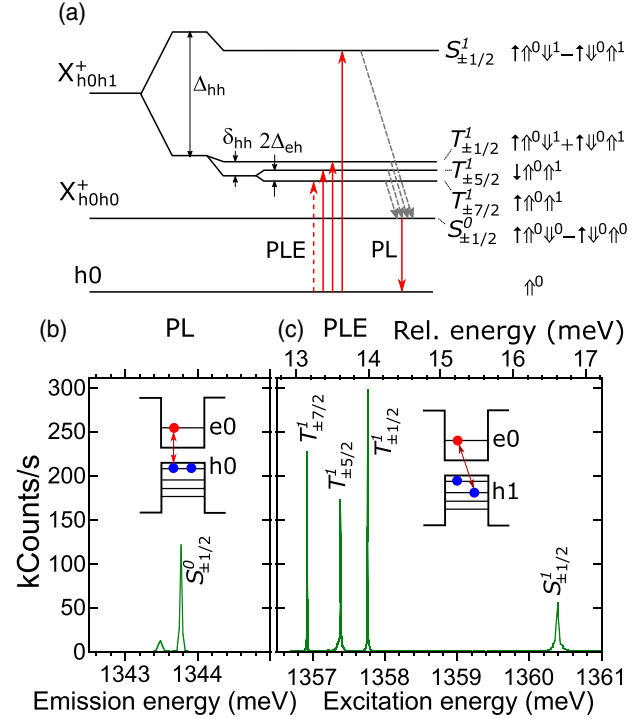


FIG. 2. (a) Energy level diagram of a QD charged with a hole, showing optical transitions to the singlet and triplet hot trions $X_{h_0h_1}^+$, nonradiative relaxation to the lowest energy trion $X_{h_0h_0}^+$, and emission to the ground state h_0 . (b) Photoluminescence (PL) emission spectrum at $B = 0$ T for the lowest energy trion $X_{h_0h_0}^+$. (c) PLE spectrum of $X_{h_0h_1}^+$ at $B = 0$ T, collecting emission from $X_{h_0h_0}^+$, with a laser power of 1μ W. Schematics of the QD electron and hole energy levels showing occupation are inset in (b) and (c).

to higher hole states (h_2, h_3). We note that none of these transitions should be allowed for p -like h_1 and s -like e_0 , due to zero electron-hole overlap, indicating mixed symmetry of orbitals [38,39]. Also, the $T_{\pm 7/2}^1$ transitions are nominally forbidden by spin selection rules since they do not change the spin projection by $\Delta m_f = \pm 1$. These “dark” trions have been observed in previous studies as well [33,34].

More insight into these transitions is obtained by applying a magnetic field along the growth direction and optical axis (Faraday geometry). Figure 3(a) displays spectrally resolved resonance fluorescence of $X_{h_0h_0}^+$ at $B = 1.5$ T when driving the $\uparrow^0 - S_{+1/2}^0$ and $\downarrow^0 - S_{-1/2}^0$ transitions resonantly. Spectra are taken near the single hole stability edge for fast hole spin relaxation to prevent optical pumping. When driving one transition, there is no sign of emission from the other allowed transition or from forbidden cross transitions (e.g., $\uparrow^0 - S_{-1/2}^0$), indicating these transitions preserve spin (cycling transitions).

In Fig. 3(b), the PLE of the triplet transitions is displayed at $B = 2$ T for σ^+ and σ^- excitation, integrating emission from both $S_{\pm 1/2}^0$ lines. Both the $T_{\pm 7/2}^1$ and $T_{\pm 5/2}^1$ transitions

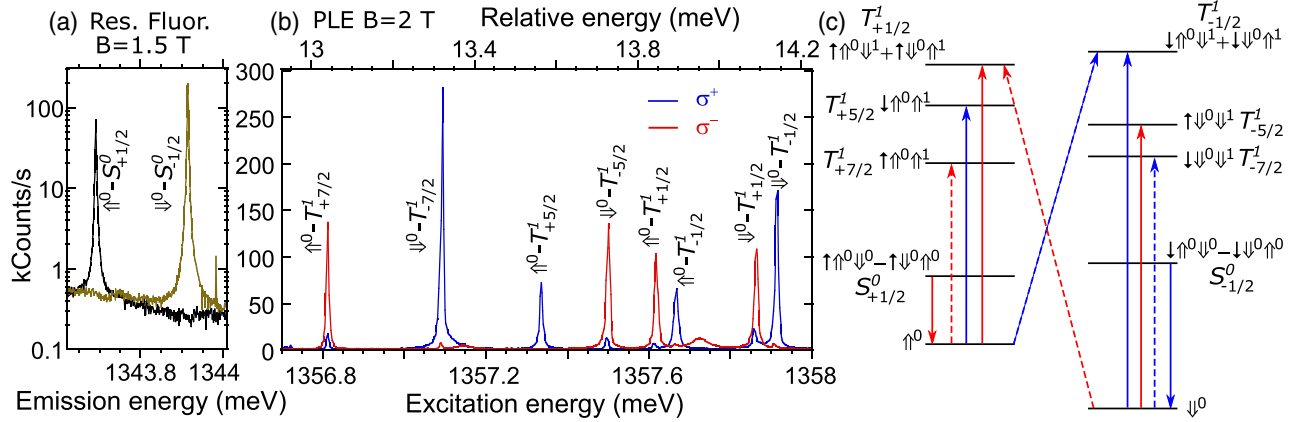


FIG. 3. (a) Spectrally resolved resonance fluorescence of $X_{h_0 h_0}^+$ at $B = 1.5$ T with the laser linearly polarized at a power of 10 nW. (b) PLE of the triplet transitions at $B = 2.0$ T, collecting light from both emission lines of $X_{h_0 h_0}^+$, for σ^+ and σ^- excitation polarizations at $1 \mu\text{W}$. The sample is biased at $V_{\text{bias}} = -0.95$ V at the charge stability edge for (a) and (b). (c) Energy level diagram showing the triplets and the lowest energy singlets, with red (σ^-) and blue (σ^+) arrows showing the expected (solid) and unexpected (dashed) optically allowed transitions.

split into two lines with opposite circular polarizations while $T_{\pm 1/2}^1$ splits into four lines, with two lines σ^+ and two lines σ^- . The energy level diagram in Fig. 3(c) displays all of these transitions. Four transitions (solid lines) are expected from spin selection rules in which a spin $\pm 1 e_0 h_1$ exciton ($\downarrow \uparrow^1$ or $\uparrow \downarrow^1$) is generated with σ^\pm polarization in addition to the resident h_0 hole. The four unexpected transitions (dashed lines) correspond to generating a spin $\pm 2 e_0 h_1$ exciton ($\uparrow \uparrow^1$ or $\downarrow \downarrow^1$) with σ^\mp polarization. This provides a σ^+ Λ system for $T_{-1/2}^1$ and a σ^- Λ system for $T_{+1/2}^1$. The double Λ system also occurs for $S_{\pm 1/2}^1$ (not shown). Moreover, a similar transition pattern occurs for the next higher shell trion ($X_{h_0 h_2}^+$). This pattern has been observed in all three QDs measured.

The unexpected transitions that give rise to the double Λ system are allowed due to spin-orbit coupling that is strong for h_1 and weak for h_0 (see Supplemental Material [25]). The spin-orbit coupling can be understood in terms of an effective magnetic field due to motion in the confinement potential [40]. The in-plane component of the effective magnetic field is responsible for spin mixing combined with orbital mixing. The state of the predominantly h_1 spin-up state can thus be written as $|\uparrow_i^1\rangle = \alpha |h_1\rangle |\uparrow\rangle + \sum_{i>1} \beta_i |h_i\rangle |\downarrow\rangle$, where $|h_i\rangle$ are the orbital states, $|\uparrow\rangle$ and $|\downarrow\rangle$ are pseudospin states, and α is expected to be nearly 1. This “tilted” spin $|\uparrow_i^1\rangle$ explains all of the unexpected transitions and their polarizations in Fig. 3(c). For example, the triplet state $(\uparrow \uparrow^0 \downarrow^1 + \uparrow \downarrow^0 \uparrow^1)/\sqrt{2}$ is given a small component $\uparrow \downarrow^0 \downarrow^i$, with one hole in an excited orbital, by substituting $\uparrow^1 \rightarrow \alpha \uparrow^1 + \beta \downarrow^i$ in the second term. This makes the transition from the ground state \downarrow^0 allowed with σ^- polarization, as observed. Other forbidden transitions that are not observed (e.g., \downarrow^0 to $\downarrow \uparrow^0 \uparrow^1$) should still be very weak since they require a

spin mixing in h_0 . We also note that even with $\beta_i \ll 1$, there can be a strong effect on the optical transitions due to changes in the electron-hole overlap. The overlap is weak for the nominally odd parity h_1 but can be much larger for even parity orbitals (e.g., h_3) that are mixed in, amplifying the effect of the spin mixing terms on optical transitions. From symmetry arguments and energy separations, we expect that the dominant mixing term is with h_3 , a nominally even parity d orbital with two nodes along the same axis as h_1 [25].

There is also an effective spin-orbit magnetic field component along the growth direction (z) that results in spin-dependent mixing of orbitals, h_1 and h_2 (p_x and p_y), while preserving the spin projection along z [41]. This does not tilt the spin and change spin selection rules, but it does result in an anisotropic hole-hole exchange interaction [41,42]. This leads to a shift of $T_{\pm 5/2}^1$ and $T_{\pm 7/2}^1$ down in energy more than $T_{\pm 1/2}^1$, resulting in the relative anisotropic exchange shift (δ_{hh}) observed in Fig. 2.

We have shown that the strong spin-orbit interactions of the excited hole in the hot trion gives the double Λ system missing in the Faraday geometry. Next, we show that this double Λ system can be used to control the ground state hole spin, starting with the ability to optically pump into a particular spin ground state. When driving a particular trion transition, optical spin pumping occurs when relaxation of the trion has some chance of returning the system to the opposite hole spin state being driven. This can happen with any of the transitions in Fig. 3(c), including the lowest energy singlet $S_{\pm 1/2}^0$, though slowly [8]. We obtain *fast* optical pumping using the new transitions in the trion triplet. In Fig. 4, we focus on the Λ system formed with $T_{-1/2}^1$ and measure time-resolved optical pumping.

The hole spin state is first randomized by pulsed excitation for 30 ns with linearly polarized light at

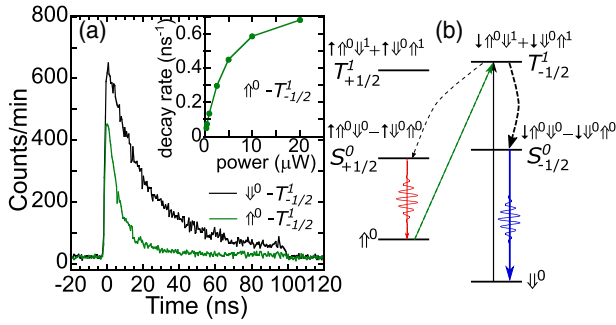


FIG. 4. (a) Time-correlated photon counting of a 100 ns pulse exciting two triplet transitions, with $B = 1.5$ T and $V_{\text{bias}} = -0.97$ V. Emission is collected from $S_{-1/2}^0$. The inset plots the decay rate as a function of drive power for the $\uparrow^0 - T_{-1/2}^1$ transition. (b) Energy level diagram showing excitation of $T_{-1/2}^1$ by either of two transitions, followed by nonradiative relaxation (curved dashed arrows), primarily to $S_{-1/2}^0$, and then emission into \downarrow^0 .

1388 meV, where transitions are broad enough to excite both hole spin states. Then a 100 ns pulse excites one of the triplet transitions. Figure 4(a) displays the time-correlated photon counting of emission from $S_{-1/2}^0$ during this pulse for excitation of the $\uparrow^0 - T_{-1/2}^1$ and $\downarrow^0 - T_{-1/2}^1$ transitions. The emission turns on rapidly with the pulse, followed by an exponential decay to nearly zero as the hole spin is pumped. At a peak power of $1 \mu\text{W}$, the decay time constants are 7.3 and 20.5 ns for the $\uparrow^0 - T_{-1/2}^1$, and $\downarrow^0 - T_{-1/2}^1$ transitions, with initialization fidelities of 99% and 97%, respectively [25]. The difference in peak intensities is attributed to the relative oscillator strengths. The differences in the decay times can be explained by the trion relaxation processes illustrated in Fig. 4(b), in which $T_{-1/2}^1$ primarily relaxes to $S_{-1/2}^0$, followed by emission to \downarrow^0 (see Supplemental Material [25]). Driving $\uparrow^0 - T_{-1/2}^1$ is thus more likely to change the spin state than driving $\downarrow^0 - T_{-1/2}^1$. As the excitation power is increased to saturation [see inset of Fig. 4(a)], the pumping time through the $\uparrow^0 - T_{-1/2}^1$ transition is only 1.5 ns, comparable to s -shell trion pumping times in the Voigt geometry [1] and about 3 orders of magnitude shorter than s -shell pumping times in the Faraday geometry [8].

With a double Λ system in the $T_{\pm 1/2}^1$ states, coherent control of the hole spin now becomes possible in the Faraday geometry. In Fig. 5 we demonstrate CPT through the trion triplet. This experiment was done on a different QD from the same sample that shows very similar behavior to that measured in Figs. 2–4 (see Supplemental Material [25]). As shown in Figs. 5(a) and 5(b), a pump laser is tuned to the $\downarrow^0 - T_{-1/2}^1$ transition and a weaker sideband probe is tuned near the $\uparrow^0 - T_{-1/2}^1$ transition, generated by an electro-optic phase modulator. Emission from $\downarrow^0 - S_{-1/2}^0$ is plotted vs the probe detuning in Fig. 5(c) for a series of pump powers. The dip observed at $40.5 \mu\text{eV}$ corresponds to the formation of a dark state when the

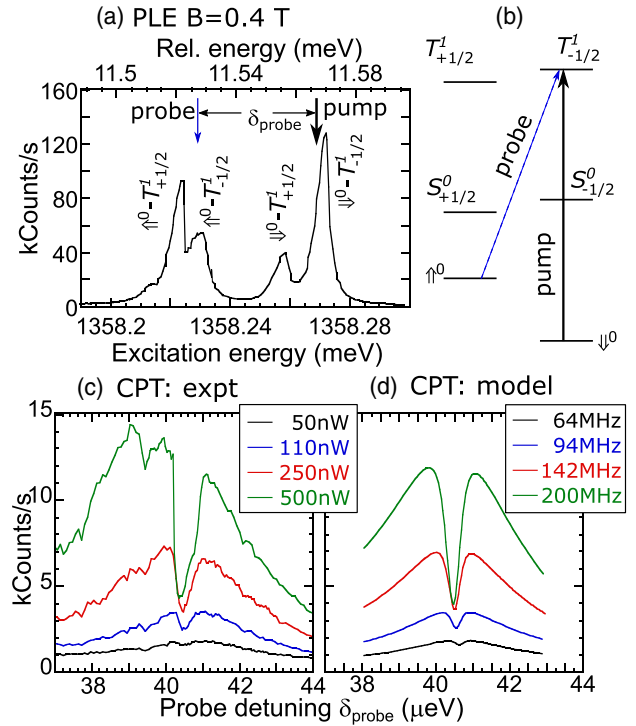


FIG. 5. (a) PLE spectrum of $T_{\pm 1/2}^1$ at $B = 0.4$ T for the second QD, using linearly polarized excitation at $0.6 \mu\text{W}$. The bias is set to the stability edge for fast hole spin relaxation. (b) Energy level diagram showing the pump and probe driving the $T_{-1/2}^1$ Λ system. (c) CPT measurements for a series of pump powers at a bias 30 mV away from the stability edge, where hole spin relaxation is much slower. Both pump and probe are polarized σ^+ . The arrows in (a) indicate the positions of the pump and probe, correcting for the Stark shift between the two biases. (d) CPT model for a series of Rabi frequencies matching experiment.

frequency difference is equal to the ground state hole spin splitting. This dark state consists of a superposition of \uparrow^0 and \downarrow^0 with coefficients determined by $\Omega_{\text{pump}}/\Omega_{\text{probe}}$, the ratio of Rabi frequencies [43]. The probe power, which varies some with the modulation frequency, is about 7% of the pump power, giving an estimate of $\Omega_{\text{probe}} = \Omega_{\text{pump}}/4$. To observe a strong CPT dip, $\Omega_{\text{pump}}^2/\Gamma \gg 1/T_2^*$, where Γ is the excited state relaxation rate and T_2^* is the spin coherence time. We numerically model the CPT data using a three-level Λ system [25,44,45], which includes spectral wandering by weighted averages over variations in the spin splitting and excited state energy. The model calculations in Fig. 5(d), taken at the experimentally determined values of Ω_{pump} [25], fit the experimental data quite well at low powers. At higher powers, the dip appears to have relatively sharp edges, and the broad peak has redshifted a little, which both likely come from nuclear polarization effects that are not captured in the model [46]. This model gives a T_2^* of about 9 ns, which is short compared to similar measurements in the Voigt geometry with $T_2^* > 100$ ns [6,7]. To our knowledge, no measurements of the hole spin

T_2^* for InAs QDs have been performed in the Faraday geometry, in which holes have a very different g factor and the hyperfine interaction is stronger [7,20], so further study is needed to characterize and understand this behavior.

This Letter demonstrates that hot trion states provide additional energy levels for control and readout of spin. In particular, the triplet $T_{\pm 1/2}^1$ states provide a double Λ system in a Faraday magnetic field, due to spin-forbidden transitions that are consistently allowed. These transitions arise from tilting of the excited hole spin by the spin-orbit interaction and occur for typical QD samples without using any special techniques. Using this system, we demonstrate fast initialization and CPT, while also showing that the lowest trion transitions strongly preserve spin. This addresses the long-standing challenge in QDs of combining efficient spin readout with fast, coherent spin control in one geometry. These higher energy transitions also have the important advantage of being spectrally separated from the emission, eliminating laser scatter with spectral filtering.

This work was supported by the U.S. Office of Naval Research, the Defense Threat Reduction Agency (Grant No. HDTRA1-15-1-0011), and the Air Force Office of Scientific Research (Grant No. FA9550-AFOSR-17RYCOR500).

*sam.carter@nrl.navy.mil

†Present address: Air Force Office of Scientific Research, Arlington, VA 22203, USA.

- [1] X. Xu, Y. Wu, B. Sun, Q. Huang, J. Cheng, D. G. Steel, A. S. Bracker, D. Gammon, C. Emary, and L. J. Sham, Fast Spin State Initialization in a Singly Charged InAs-GaAs Quantum Dot by Optical Cooling, *Phys. Rev. Lett.* **99**, 097401 (2007).
- [2] D. Press, T. D. Ladd, B. Zhang, and Y. Yamamoto, Complete quantum control of a single quantum dot spin using ultrafast optical pulses, *Nature (London)* **456**, 218 (2008).
- [3] J. Berezovsky, M. Mikkelsen, N. Stoltz, L. Coldren, and D. Awschalom, Picosecond coherent optical manipulation of a single electron spin in a quantum dot, *Science* **320**, 349 (2008).
- [4] X. Xu, B. Sun, P. R. Berman, D. G. Steel, A. S. Bracker, D. Gammon, and L. J. Sham, Coherent population trapping of an electron spin in a single negatively charged quantum dot, *Nat. Phys.* **4**, 692 (2008).
- [5] D. Brunner, B. D. Gerardot, P. A. Dalgarno, G. Wüst, K. Karrai, N. G. Stoltz, P. M. Petroff, and R. J. Warburton, A coherent single-hole spin in a semiconductor, *Science* **325**, 70 (2009).
- [6] J. Houel, J. H. Prechtel, A. V. Kuhlmann, D. Brunner, C. E. Kuklewicz, B. D. Gerardot, N. G. Stoltz, P. M. Petroff, and R. J. Warburton, High Resolution Coherent Population Trapping on a Single Hole Spin in a Semiconductor Quantum Dot, *Phys. Rev. Lett.* **112**, 107401 (2014).
- [7] J. H. Prechtel, A. V. Kuhlmann, J. Houel, A. Ludwig, S. R. Valentin, A. D. Wieck, and R. J. Warburton, Decoupling a hole spin qubit from the nuclear spins, *Nat. Mater.* **15**, 981 (2016).
- [8] A. Delteil, W. B. Gao, P. Fallahi, J. Miguel-Sanchez, and A. Imamoglu, Observation of Quantum Jumps of a Single Quantum Dot Spin Using Submicrosecond Single-Shot Optical Readout, *Phys. Rev. Lett.* **112**, 116802 (2014).
- [9] S. G. Carter, T. M. Sweeney, M. Kim, C. S. Kim, D. Solenov, S. E. Economou, T. L. Reinecke, L. Yang, A. S. Bracker, and D. Gammon, Quantum control of a spin qubit coupled to a photonic crystal cavity, *Nat. Photonics* **7**, 329 (2013).
- [10] S. Sun, H. Kim, G. S. Solomon, and E. Waks, Cavity-Enhanced Optical Readout of a Single Solid-State Spin, *Phys. Rev. Applied* **9**, 054013 (2018).
- [11] S. Sun, H. Kim, Z. Luo, G. S. Solomon, and E. Waks, A single-photon switch and transistor enabled by a solid-state quantum memory, *Science* **361**, 57 (2018).
- [12] M. H. Appel, A. Tiranov, A. Javadi, M. C. Löbl, Y. Wang, S. Scholz, A. D. Wieck, A. Ludwig, R. J. Warburton, and P. Lodahl, A Coherent Spin-Photon Interface with Waveguide Induced Cycling Transitions, *Phys. Rev. Lett.* **126**, 013602 (2021).
- [13] T. A. Wilkinson, D. J. Cottrill, J. M. Cramlet, C. E. Maurer, C. J. Flood, A. S. Bracker, M. Yakes, D. Gammon, and E. B. Flagg, Spin-selective AC Stark shifts in a charged quantum dot, *Appl. Phys. Lett.* **114**, 133104 (2019).
- [14] H. Kosaka, H. Shigyou, Y. Mitsumori, Y. Rikitake, H. Imamura, T. Kutsuwa, K. Arai, and K. Edamatsu, Coherent Transfer of Light Polarization to Electron Spins in a Semiconductor, *Phys. Rev. Lett.* **100**, 096602 (2008).
- [15] Y. H. Huo, B. J. Witek, S. Kumar, J. R. Cardenas, J. X. Zhang, N. Akopian, R. Singh, E. Zallo, R. Grifone, D. Krieger, R. Trotta, F. Ding, J. Stangl, V. Zwiller, G. Bester, A. Rastelli, and O. G. Schmidt, A light-hole exciton in a quantum dot, *Nat. Phys.* **10**, 46 (2014).
- [16] G. Éthier-Majcher, P. St-Jean, and S. Francoeur, Light- and heavy-hole trions bound to isoelectronic centers, *Phys. Rev. B* **92**, 155436 (2015).
- [17] D. Kim, S. Economou, Ş. Bădescu, M. Scheibner, A. Bracker, M. Bashkansky, T. Reinecke, and D. Gammon, Optical Spin Initialization and Nondestructive Measurement in a Quantum Dot Molecule, *Phys. Rev. Lett.* **101**, 236804 (2008).
- [18] A. N. Vamivakas, C.-Y. Lu, C. Matthesen, Y. Zhao, S. Fält, A. Badolato, and M. Atatüre, Observation of spin-dependent quantum jumps via quantum dot resonance fluorescence, *Nature (London)* **467**, 297 (2010).
- [19] S. T. Yilmaz, P. Fallahi, and A. Imamoglu, Quantum-Dot-Spin Single-Photon Interface, *Phys. Rev. Lett.* **105**, 033601 (2010).
- [20] J. Fischer, W. Coish, D. Bulaev, and D. Loss, Spin decoherence of a heavy hole coupled to nuclear spins in a quantum dot, *Phys. Rev. B* **78**, 155329 (2008).
- [21] P. Fallahi, S. T. Yilmaz, and A. Imamoglu, Measurement of a Heavy-Hole Hyperfine Interaction in InGaAs Quantum Dots Using Resonance Fluorescence, *Phys. Rev. Lett.* **105**, 257402 (2010).
- [22] A. Greilich, S. G. Carter, D. Kim, A. S. Bracker, and D. Gammon, Optical control of one and two hole spins in interacting quantum dots, *Nat. Photonics* **5**, 702 (2011).

- [23] K. De Greve, P.L. McMahon, D. Press, T.D. Ladd, D. Bisping, C. Schneider, M. Kamp, L. Worschech, S. Höfling, A. Forchel, and Y. Yamamoto, Ultrafast coherent control and suppressed nuclear feedback of a single quantum dot hole qubit, *Nat. Phys.* **7**, 872 (2011).
- [24] S.G. Carter, S.E. Economou, A. Greilich, E. Barnes, T. Sweeney, A.S. Bracker, and D. Gammon, Strong Hyperfine-Induced Modulation of an Optically-Driven Hole Spin in an InAs Quantum Dot, *Phys. Rev. B* **89**, 075316 (2014).
- [25] See Supplemental Material at <http://link.aps.org/supplemental/10.1103/PhysRevLett.126.107401> for details on the sample structure, PLE from a second QD, theory of spin-orbit mixing, triplet pumping times, measurements of the Rabi frequency, and the coherent population trapping model, which includes Refs. [26–29].
- [26] Y. Léger, L. Besombes, L. Maingault, and H. Mariette, Valence-band mixing in neutral, charged, and Mn-doped self-assembled quantum dots, *Phys. Rev. B* **76**, 045331 (2007).
- [27] K. Kowalik, O. Krebs, A. Golnik, J. Suffczyński, P. Wojnar, J. Kossut, J. A. Gaj, and P. Voisin, Manipulating the exciton fine structure of single CdTe ZnTe quantum dots by an in-plane magnetic field, *Phys. Rev. B* **75**, 195340 (2007).
- [28] K. Kowalik, O. Krebs, A. Lemaître, J. A. Gaj, and P. Voisin, Optical alignment and polarization conversion of the neutral-exciton spin in individual InAs/GaAs quantum dots, *Phys. Rev. B* **77**, 161305(R) (2008).
- [29] A. V. Koudinov, I. A. Akimov, Y. G. Kusrayev, and F. Henneberger, Optical and magnetic anisotropies of the hole states in Stranski-Krastanov quantum dots, *Phys. Rev. B* **70**, 241305(R) (2004).
- [30] J. Dreiser, M. Atatüre, C. Galland, T. Müller, A. Badolato, and A. Imamoglu, Optical investigations of quantum dot spin dynamics as a function of external electric and magnetic fields, *Phys. Rev. B* **77**, 075317 (2008).
- [31] K. V. Kavokin, Fine structure of the quantum-dot trion, *Phys. Status Solidi A* **195**, 592 (2003).
- [32] M. E. Ware, E. A. Stinaff, D. Gammon, M. F. Doty, A. S. Bracker, D. Gershoni, V. L. Korenev, Ş. C. Bădescu, Y. Lyanda-Geller, and T. L. Reinecke, Polarized Fine Structure in the Photoluminescence Excitation Spectrum of a Negatively Charged Quantum Dot, *Phys. Rev. Lett.* **95**, 177403 (2005).
- [33] T. Warming, E. Siebert, A. Schliwa, E. Stock, R. Zimmermann, and D. Bimberg, Hole-hole and electron-hole exchange interactions in single InAs/GaAs quantum dots, *Phys. Rev. B* **79**, 125316 (2009).
- [34] E. Siebert, T. Warming, A. Schliwa, E. Stock, M. Winkelnkemper, S. Rodt, and D. Bimberg, Spectroscopic access to single-hole energies in InAs/GaAs quantum dots, *Phys. Rev. B* **79**, 205321 (2009).
- [35] V. Jovanov, S. Kapfinger, M. Bichler, G. Abstreiter, and J. J. Finley, Direct observation of metastable hot trions in an individual quantum dot, *Phys. Rev. B* **84**, 235321 (2011).
- [36] Y. Benny, Y. Kodriano, E. Poem, D. Gershoni, T. A. Truong, and P. M. Petroff, Excitation spectroscopy of single quantum dots at tunable positive, neutral, and negative charge states, *Phys. Rev. B* **86**, 085306 (2012).
- [37] M. V. Durnev, M. Vidal, L. Bouet, T. Amand, M. M. Glazov, E. L. Ivchenko, P. Zhou, G. Wang, T. Mano, N. Ha, T. Kuroda, X. Marie, K. Sakoda, and B. Urbaszek, Magneto-spectroscopy of excited states in charge-tunable GaAs/AlGaAs quantum dots, *Phys. Rev. B* **93**, 245412 (2016).
- [38] G. Bester, S. Nair, and A. Zunger, Pseudopotential calculation of the excitonic fine structure of million-atom self-assembled InGaAs/GaAs quantum dots, *Phys. Rev. B* **67**, 161306(R) (2003).
- [39] A. Schliwa, M. Winkelnkemper, and D. Bimberg, Impact of size, shape, and composition on piezoelectric effects and electronic properties of In(Ga)As/GaAs quantum dots, *Phys. Rev. B* **76**, 205324 (2007).
- [40] R. Winkler, *Spin Orbit Coupling Effects in Two-Dimensional Electron and Hole Systems* (Springer, New York, 2003).
- [41] Ş. C. Bădescu and T. L. Reinecke, Mixing of two-electron spin states in a semiconductor quantum dot, *Phys. Rev. B* **75**, 041309(R) (2007).
- [42] K. V. Kavokin, Symmetry of anisotropic exchange interactions in semiconductor nanostructures, *Phys. Rev. B* **69**, 075302 (2004).
- [43] D. A. Steck, Quantum and Atom Optics, available online at <http://steck.us/teaching> (revision 0.8.3, 2012).
- [44] J. R. Johansson, P. D. Nation, and F. Nori, QuTiP: An open-source Python framework for the dynamics of open quantum systems, *Comput. Phys. Commun.* **183**, 1760 (2012).
- [45] J. R. Johansson, P. D. Nation, and F. Nori, QuTiP 2: A Python framework for the dynamics of open quantum systems, *Comput. Phys. Commun.* **184**, 1234 (2013).
- [46] X. Xu, W. Yao, B. Sun, D. G. Steel, A. S. Bracker, D. Gammon, and L. J. Sham, Optically controlled locking of the nuclear field via coherent dark-state spectroscopy, *Nature (London)* **459**, 1105 (2009).